Int. J. Electrochem. Sci., 12 **(2017)** 1774 – 1784, doi: 10.20964/2017.03.68

International Journal of ELECTROCHEMICAL SCIENCE
www.electrochemsci.org

An Electrochemical Study of Pyrite Oxidation in 0.1 M Sulfuric Acid at High Temperature and High Pressure

Sen Lin, Heping Li[*]*, Liping Xu, Li Zhou, Can Cui*

Key Laboratory for High Temperature & High Pressure Study of the Earth's Interior, Institute of Geochemistry, Chinese Academy of Sciences, Guiyang, 550081, China
[*]E-mail: liheping@vip.gyig.ac.cn

Received: 1 November 2016 / *Accepted:* 23 January 2017 / *Published:* 12 February 2017

Open circuit potential, potentiodynamic polarization plots and electrochemical impedance spectroscopy for pyrite in 0.1 M sulfuric acid in the temperature range of 200 to 350 °C and pressure range of 25 to 40 MPa were measured, with the aid of a self-designed electrochemical measurement set-up which can operate at high temperature and high pressure. Results show that increased temperatures benefit the oxidation of pyrite: at 40 MPa, when the temperature was rised from 200 to 350 °C, corrosion potential (E_{corr}) decreased from -199.83 to -778.78 mV, corrosion current density (i_{corr}) increased from 4.33 to 22.16 mA/cm^2, polarization resistance (R_p) decreases from 34.11 to 3.85 Ω·cm^2, resistance of the passive layer (R_{pl}) decreased from 42.16 to 2.48 Ω·cm^2. Effects of pressure were also considered, at 300 °C, when pressure was increased from 25 to 40 MPa, E_{corr} decreased from -621.48 to -713.25 mV, however, i_{corr} and R_p rarely changed.

Keywords: Pyrite; acid pressure oxidation; open circuit potential; potentiodynamic polarization; electrochemical impedance spectroscopy

1. INTRODUCTION

Pyrite, the most common iron sulfide mineral, is rarely of economic value. However, it often appears together with other valuable metal minerals, gold for example. Refractory gold is often found finely disseminated in the lattice of pyrite [1], acid pressure oxidation at high temperatures [2] is an effective method to break down the pyrite lattice and enhance gold collection in the following cyanidation.

Acid pressure oxidation of pyrite has been practiced commercially since 1980s [3], much research has been performed in this field. Acid pressure oxidation of pyrite, which is controlled by

surface reaction rate [4], involves a series of complex reactions to produce ferrous and ferric ions, sulfate ions, and elemental sulfur [5]. The relevant amount of the products are determined by applied conditions, such as temperature, acidity, and oxygen partial pressure. Baily and Peters [6] studied the acid pressure oxidation of pyrite at 85 to 130 °C, they convincingly demonstrated that the acid pressure oxidation of pyrite was an electrochemical process, and the anodic reaction could be represented by the two competing reactions:

$$FeS_2 + 8H_2O \rightarrow Fe^{2+} + 2SO_4^{2-} + 16H^+ + 14e^-$$

$$FeS_2 \rightarrow Fe^{2+} + 2S + 2e^-$$

They also claimed that at temperatures exceeding the melting point of elemental sulfur, a liquid sulfur passive film enveloped the pyrite surface, resulting in cease of the oxidation after about 65% conversion. Papangelakis and Demopoulos [7] investigated the acid pressure oxidation of pyrite in the temperature range of 140 to 180 °C and proposed a shrinking core model to fit the reaction kinetics, they also found that the acid pressure oxidation of pyrite completed only at temperatures above 160 °C. Long and Dixon [4] studied the acid pressure oxidation of pyrite at 170 – 230 °C, they claimed that the reaction mechanism was electrochemical, and ferric ion was the initial product of the reaction, a passivating shrinking sphere model was proposed to fit the reaction kinetics in their work.

In previous studies, researchers investigated the acid pressure oxidation of pyrite mainly by examining the changes in the amount of reactants and products after the system was cooling down, reaction kinetics and mechanism were then deduced from such information. However, the method is unsatisfactory in some ways. Firstly, the method is ex-situ, researchers measured the amount of reactants and products after cooling down, it is hard to quantify variation in the amount of reactants and products that may take place in the cooling process, which introduces uncertain errors to the experimental results; secondly, solid-liquid interface is the place where pyrite oxidation takes place, information of such interface is crucial in understanding the reaction mechanism, unfortunately, the previous method gave little information about this interface.

Considering the limiting of the previous research method, an informative and accurate in-situ research technique is quite necessary. Electrochemical measurement technique is a powerful tool in the oxidation research of materials, which has already been widely employed in pyrite oxidation research at room temperature [8-11]. Given that it is well accepted by researchers that the mechanism of pyrite acid pressure oxidation is electrochemical [4, 6], it is feasible to study the acid pressure oxidation of pyrite with electrochemical measurement technique in principle. The application of electrochemical measurement technique at high temperature and high pressure appeares mainly in corrosion studies of metallic materials [12-14]. Unfortunately, limited by experimental technique, there was no report of three-electrode electrochemical investigation into pyrite acid pressure oxidation at temperatures above 200 °C so far.

In this work, electrochemical investigation of pyrite acid pressure oxidation in 0.1 M sulfuric acid was performed in the temperature range of 200 to 350 °C and pressure range of 25 to 40 MPa, with the aid of a self-designed experimental set-up for three-electrode electrochemical measurement in high temperature and high pressure fluids. The effects of temperature and pressure on pyrite acid pressure oxidation behaviors were studied by the measurements of open circuit potential (OCP), potentiodynamic polarization and electrochemical impedance spectroscopy (EIS).

2. EXPERIMENTAL

The experimental set-up used in this work was detailed described in another paper of our group [15]. In this set-up, the electrodes are sealed by pyrophyllite taper sleeve with a conical self-energizing sealing structure, this design enables the set-up to employ fragile material as working electrode.

The working electrode in this work was a pyrite cone frustum, which was made from a big monocrystal pyrite with the aid of a lathe. The counter electrode was a self-made alumina ceramic cone frustum with a platinum wire inside, platinum power was sintered on the round surface of the ceramic to achieve sufficient counter electrode surface area. An external pressure-balanced Ag/AgCl electrode filled with 0.1 M KCl was utilized as the reference electrode. In present work, the calibrated equation of the electrode potential was following [16]:

$$\Delta E_{SHE} = \Delta E_{obs} + 286.6 - \Delta T + 1.745 \times 10^{-4}\Delta T^2 - 3.03 \times 10^{-6}\Delta T^3 \text{ (mV)}$$

All potentials mentioned in this work are normalized with respect to the saturated hydrogen electrode (SHE) using the formula above. The pyrite working electrode was primarily abraded with 1000, 2000, and 2500-grit SiC paper in turn, then washed by alcohol and deionized water. Silver conductive paste that can be used at high temperatures was employed to connect the electrodes with silver wires. All conducting wires were isolated by alumina ceramic tubes.

To avoid the oxidation of pyrite when heated, high purity argon was introduced into the autoclave to drive the air out before heating. As the autoclave was heated to the set temperature, 1 mL 30% hydrogen peroxide and proper amount of 0.1 M sulfuric acid were pumped into the autoclave using a pressure pump, until the pressure reached the desired value. When hydrogen peroxide was pumped into the hot autoclave, it decomposed into oxygen and water immediately:

$$2H_2O_2 \rightarrow 2H_2O + O_2$$

To make sure that all oxygen dissolve in the solution, the pressure in the experiments was set not less than 25 MPa [17], the oxygen concentration in all experiments was 0.16 mol/L.

Electrochemical measurements were conducted using a Princeton 2263A electrochemical test station and Powersuit software. EIS studies at open circuit potential were performed 5 minutes after the solutions was pumped in, the frequency was ranged from 100 kHz to 100 mHz, and the AC amplitude was 10 mV. Potentiodynamic polarization plots were measured after the EIS tests, the scan was ranged from -250 to 250 mV relative to the open circuit potential at a scan rate of 1 mV/s. Software ZSimpWin and CorrView were employed to fit the EIS and potentiodynamic polarization data, respectively. All chemical reagents used in this work were of analytical grade.

3. RESULTS AND DISCUSSION

3.1 Effects of temperature

Fig.1 shows the open circuit potential of the pyrite electrode at 200, 250, 300 and 350 °C, when the pressure is 40 MPa. It can be seen that the open circuit potential decreases with increasing

temperatures. As the temperature increases from 200 to 350 °C, the open circuit potential decreases from -189.5 to -771.8 mV. According to Gibbs-Helmholtz equation:

$$\left(\frac{\partial \Delta G}{\partial \Delta T}\right)_P = -\Delta S$$

While, $\Delta G = -nEF$

Thus, $\Delta S = nF\left(\frac{\partial \Delta E}{\partial \Delta T}\right)_P$

$$Q = T\Delta S = nFT\left(\frac{\partial \Delta E}{\partial \Delta T}\right)_P$$

where ΔG is Gibbs free energy change, ΔS is reaction entropy change, T is temperature, P is pressure, n is number of electron transfer, E is electrode potential, F is Faraday constant, Q is reaction heat. $\left(\frac{\partial \Delta E}{\partial \Delta T}\right)_P$ represents the change in electrode potential with temperature when the pressure is constant, it is negative in this work, thus, the reaction heat Q is also negative, indicating the acid pressure oxidation of pyrite is an exothermic reaction.

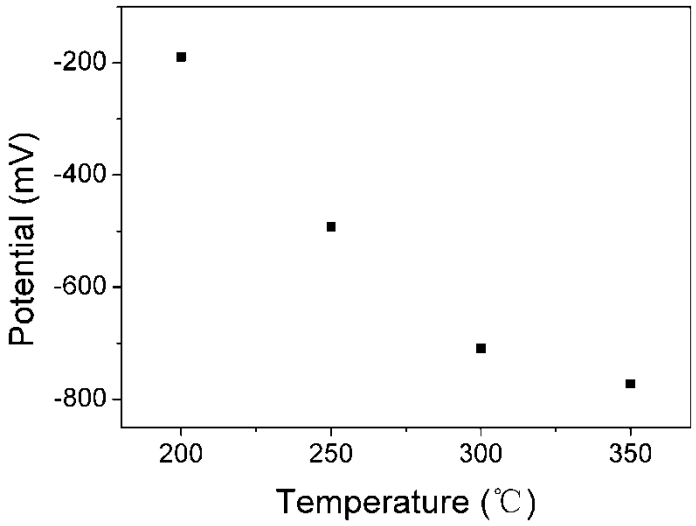

Figure 1. Open circuit potential for pyrite in 0.1 M sulfuric acid at different temperatures when the pressure is 40 MPa.

The potentiodynamic polarization plots for pyrite in 0.1 M sulfuric acid in the temperature range of 200 to 350 °C at 40 MPa are shown in Fig. 2. It can be seen that the corrosion potential decreases with the increased temperatures, whereas the current density increases with the increased temperatures. Linear fitting was performed in the potential range of E_{corr} – 200 mV to E_{corr} – 100 mV for the cathodic branch, and E_{corr} + 100 mV to E_{corr} + 200 mV for the anodic branch. In the selected potential range, the polarization plots show good linearity, indicating that the reaction is under electrochemical control. Electrochemical kinetic parameters such as corrosion potential (E_{corr}), corrosion current density (i_{corr}), and Tafel slope (β_a, β_c) were obtained through Tafel fitting. Transfer

coefficient (α), number of electrons transferred in the rate-determining step (n) and polarization resistance (R_p) were also calculated using the Bulter-Volmer equation [18] and the Tafel slopes obtained by Tafel fitting. The results are presented in Table. 1.

Table 1. Electrochemical kinetic parameters of pyrite in 0.1 M sulfuric acid in the temperature range of 200 to 350 °C at 40 MPa.

Temperature (°C)	E_{corr} (mV)	i_{corr} (mA/cm^2)	β_a (mV/decade)	β_c (mV/decade)	R_p (Ω·cm^2)	α	n
200	-197.34	4.33	209.21	502.51	34.11	0.29	0.28
250	-496.20	5.09	212.31	384.62	26.88	0.36	0.33
300	-713.25	17.63	237.53	155.44	5.33	0.61	0.52
350	-778.78	22.16	270.27	124.53	3.85	0.68	0.63

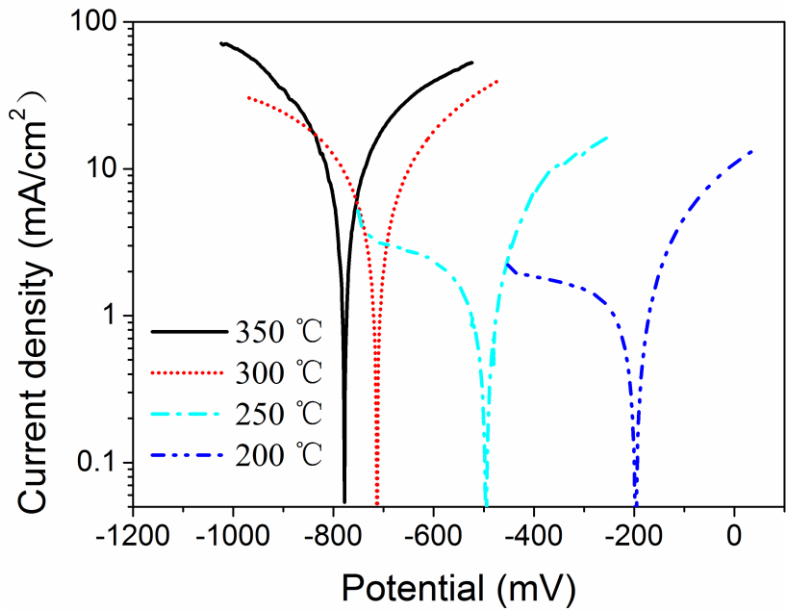

Figure 2. Potentiodynamic polarization curves for pyrite in 0.1 M sulfuric acid in the temperature range of 200 to 350 °C at 40 MPa.

As shown in Table 1, E_{corr} decreases from -199.83 to -778.78 mV when the temperature increases from 200 to 350 °C. It can be noted that, at all the studied temperatures, the value of E_{corr} is negative to the value of the open circuit potential in Fig. 1, the phenomenon can be attributed to the following two reasons: firstly, the reducing initial potential causes the change of the pyrite surface state, resulting in the negative shift of the electrode potential; secondly, the disturbance of double layer charging current in the positive scan [19]. Table 1 also shows that, as the temperature increases from 200 to 350 °C, i_{corr} increases from 4.33 to 22.16 mA/cm^2, β_a increases from 209.21 to 270.27 mV/decade, β_c decreases from 502.51 to 124.53 mV/decade, and R_p decreases from 34.11 to 3.85 Ω·cm^2. The change in i_{corr} and R_p demonstrates that increasing temperatures promote the oxidation of pyrite. Moreover, transfer coefficient (α) increases from 0.29 to 0.68, and the number of electrons

transferred in the rate-determining step (n) increases from 0.28 to 0.63 as the temperature rises from 200 to 350 °C. The change in α and n reveals different electrochemical interaction mechanisms when the temperature rises.

The average activation energy E_a for pyrite oxidation in 0.1 M sulfuric acid at 40 MPa in the temperature range of 200 to 350 °C was calculated according to Arrhenius equation. The result is 29.8 kJ/mol, which is lower than the results in literatures at lower temperatures [4, 7].

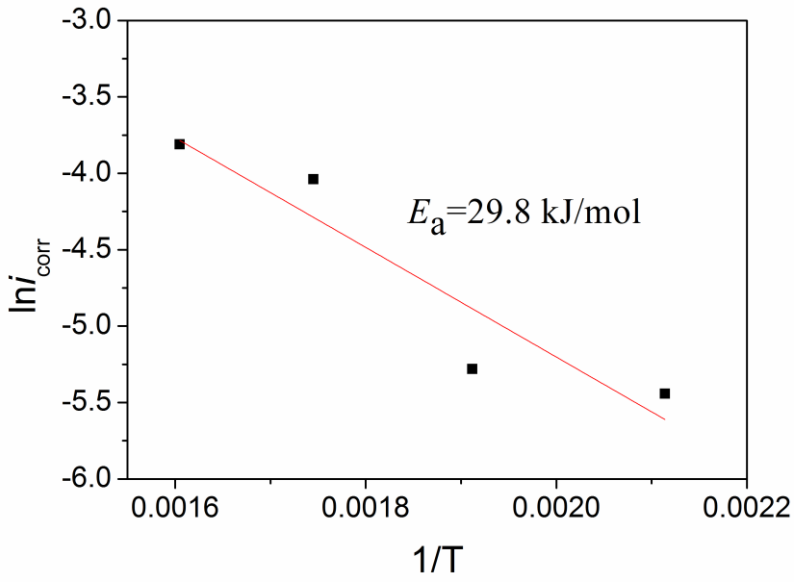

Figure 3. Arrhenius plots for pyrite in 0.1 M sulfuric acid at 40 MPa.

Fig. 4a, b, c and d shows the Bode and Nyquist plots for pyrite in 0.1 M sulfuric acid in the temperature range of 200 to 350 °C at 40 MPa. The Bode plots reveal two time constants, which are related to the capacitance and resistance of the double-layer and the passive layer at the pyrite surface, respectively. The equivalent circuit in Fig. 4e is employed to fit the experimental impedance data. In the equivalent circuit, R_s represents the ohmic resistance of the electrolyte and electrodes, Q_{ct} and R_{ct} represent the capacitance and resistance of the double-layer at pyrite surface, while, Q_{pl} and R_{pl} represent the capacitance and resistance of the passive layer. The passive layer here is the liquid elemental sulfur generated in the oxidation of pyrite [7]:

$$FeS_2 + O_2 + H_2O \rightarrow Fe^{3+} + SO_4^{2-} + S + H^+$$

Q is the constant phase angle element to replace the interfacial capacitance due to the surface roughness of the electrode [20], which is defined as [21]:

$$Q = Y_0(j\omega)^{n'} = Y_0\omega^{n'}\cos\frac{n\pi}{2} + jY_0\omega^{n'}\sin\frac{n\pi}{2}$$

where Y_0 is a constant depending on the electrode potential, and n' is the frequency power. The interfacial capacitance C can be obtained through the following equation [22]:

$$C = Y_0(\omega_m)^{n'-1}$$

ω_m is the angular frequency at which the imaginary part of the impedance has the maximum value. The results are listed in Table 2.

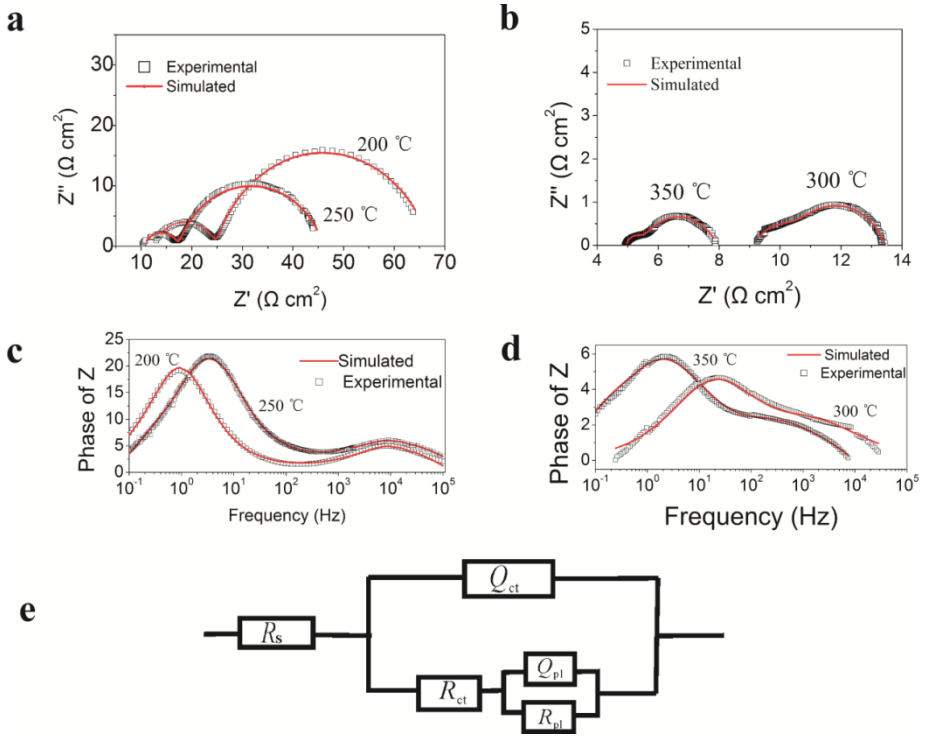

Figure 4. Nyquist plots (a), Bode plots (c) at 200 and 250 °C, Nyquist plots (b), Bode plots (d) at 300 and 350 °C and the equivalent circuit (e) for pyrite in 0.1 M sulfuric acid at 40 MPa.

Table 2. Impedance parameters of pyrite in 0.1 M sulfuric acid in the temperature range of 200 to 350 °C at 40 MPa.

Temperature (°C)	R_s ($\Omega \cdot cm^2$)	Q_{ct}			R_{ct} ($\Omega \cdot cm^2$)	Q_{pl}			R_{pl} ($\Omega \cdot cm^2$)
		Y_0	n'	C (F/cm^2)		Y_0	n'	C (F/cm^2)	
200	12.35	2.09E-5	0.72	9.67E-7	12.57	4.74E-3	0.81	3.39E-3	42.16
250	10.53	2.81E-5	0.79	2.91E-6	6.86	5.54E-3	0.77	4.14E-3	28.75
300	9.16	1.95E-3	0.62	4.00E-5	1.66	1.30E-2	0.67	6.53E-3	2.65
350	4.95	2.83E-3	0.79	7.24E-4	0.56	0.11	0.60	2.19E-2	2.48

As shown in Table 2, C of Q_{ct} increases from 9.67E-7 to 7.24E-4 F/cm^2, R_{ct} decreases from 12.57 to 0.56 Ω cm^2, C of Q_{pl} increases from 3.39E-3 to 2.19E-2 F/cm^2, and R_{pl} decreases from 42.16 to 2.48 Ω cm^2 when the temperature increases from 200 to 350 °C. The decrease in R_{ct} and the increase in C of Q_{ct} indicate that increasing temperature benefits the charge transfer step through the double-layer. While, the decrease in R_{pl} and the increase in C of Q_{pl} show that increasing temperature weakens the passive layer at the pyrite surface. Firstly, the viscosity of liquid sulfur decreases from 21.5 to 0.50 Pa · s when the temperature rises from 200 to 350 °C [23], the decrease in viscosity of liquid sulfur reduces the resistance for the mass transfer process though the passive layer; Secondly, increasing temperature accelerates the diffusion and oxidation of the liquid sulfur, reducing the thickness of the passive layer.

3.2 Effects of pressure

Fig. 5 shows the potentiodynamic polarization plots for pyrite in 0.1 M sulfuric acid in the pressure range of 25 to 40 MPa at 300 °C. The potentiodynamic polarization plots are similar in shape, but exhibit some differences in E_{corr} and Tafel slopes, the fitting results are presented in Table 3. The results show that E_{corr} decreases from -621.48 to -713.25 mV, β_a decreases from 258.40 to 237.53 mV/decade, and β_c increases from 143.88 to 155.44 mV/decade, when the pressure increases from 25 to 40 MPa. Moreover, the value of i_{corr}, transfer coefficient (α), number of electrons transferred in the rate-determining step (n) and polarization resistance (R_p) rarely change with increasing pressure.

Table 3. Electrochemical kinetic parameters of pyrite in 0.1 M sulfuric acid in the pressure range of 25 to 40 MPa at 300 °C.

Pressure (MPa)	E_{corr} (mV)	i_{corr} (mA)	β_a (mV/decade)	β_c (mV/decade)	R_p ($\Omega \cdot cm^2$)	α	n
25	-621.48	16.11	258.40	143.88	5.73	0.64	0.54
30	-649.51	15.95	253.81	144.72	5.77	0.64	0.53
35	-679.55	16.15	242.72	150.04	5.74	0.62	0.53
40	-713.25	17.63	237.53	155.44	5.33	0.61	0.52

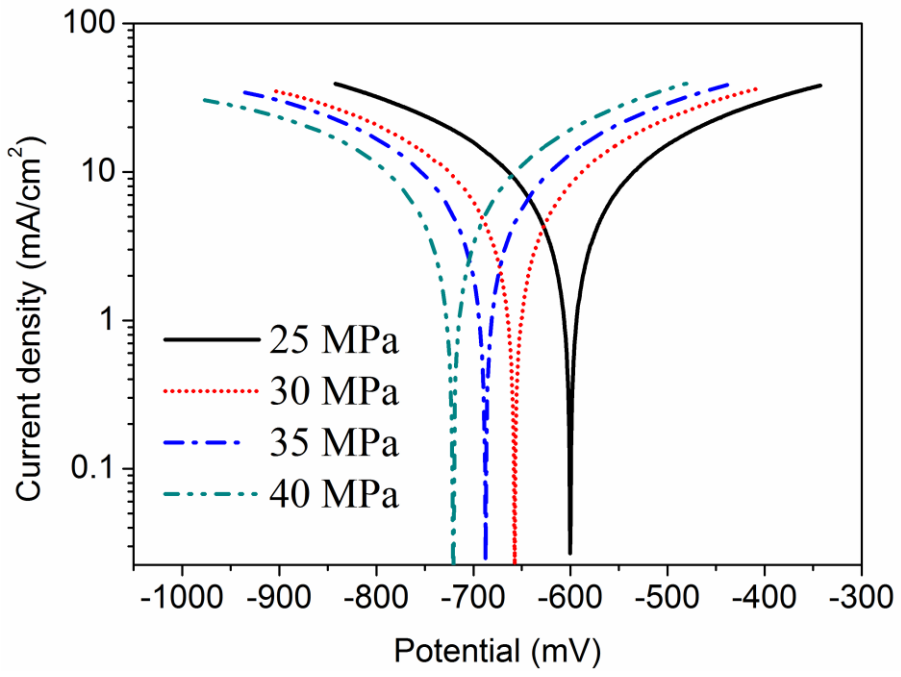

Figure 5. Potentiodynamic polarization for pyrite in 0.1 M sulfuric acid in the pressure range of 25 to 40 MPa at 300 °C.

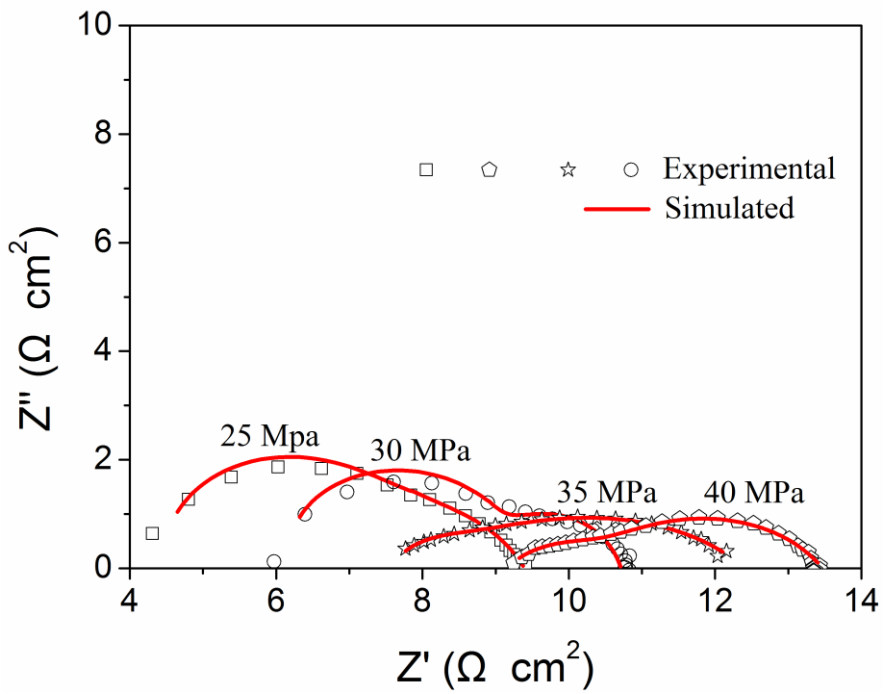

Figure 6. Nyquist plots for pyrite in 0.1 M sulfuric acid in the pressure range of 25 to 40 MPa at 300 °C.

The decrease in E_{corr} indicates that pyrite is more active at higher pressures, pyrite gains more strain energy when the pressure increases, and the strain energy changes into electrochemical energy, thereby facilitating the oxidation of pyrite [24, 25]. The almost invariable transfer coefficient (α) and number of electrons transferred in the rate-determining step (n) show a constant electrochemical interaction mechanism when the pressure changes.

EIS studies were also conducted to determine the effects of pressure on pyrite oxidation at elevated temperatures. Fig. 6 shows the Nyquist plots for pyrite in 0.1 M sulfuric acid in the pressure range of 25 to 40MPa at 300 °C, the equivalent circuit in Fig. 4e was used to fit the experimental data, and the fitting results are listed in Table 4. It can be noticed that, when the pressure increase from 25 to 40 MPa, R_{ct} decreases from 2.51 to 1.66 Ω cm^2, C of Q_{ct} decreases from 1.01E-3 to 4.00E-5 F/cm^2. While R_{pl} and C of Q_{pl} barely change with increasing pressure.

Table 4. Impedance parameters of pyrite in 0.1 M sulfuric acid in the pressure range of 25 to 40 MPa at 300 °C.

Pressure (MPa)	R_s (Ω·cm^2)	Q_{ct}			R_{ct} (Ω·cm^2)	Q_{pl}			R_{pl} (Ω·cm^2)
		Y_o	n'	C (F/cm^2)		Y_o	n'	C (F/cm^2)	
25	4.18	2.09E-3	0.82	1.01E-3	2.51	1.22E-2	0.64	6.78E-3	2.63
30	5.91	2.11E-3	0.63	1.85E-4	2.37	1.31E-2	0.62	6.51E-3	2.51
35	7.66	1.57E-3	0.74	9.49E-5	1.85	1.28E-2	0.70	6.25E-3	2.58
40	9.16	1.95E-3	0.62	4.00E-5	1.66	1.30E-2	0.67	6.53E-3	2.65

The decrease in R_{ct} shows that increasing pressures promote the charge transfer step though the double-layer. The relatively constant R_{pl} and C of Q_{pl} show that the passive film at pyrite surface is almost invariably with increasing pressures.

The potentiodynamic polarization and EIS studies show that increasing pressures decrease the corrosion potential of pyrite, which is the same as the results of metal corrosion studies in literatures [26, 27]. While, increasing pressures show little impact on the corrosion rate of pyrite. Though increasing pressures promote the charge transfer step of anodic reaction [25], meanwhile, the viscosity of the liquid sulfur passive film increases with increasing pressures, resulting in hindering of the mass transfer step through the passive film. The corrosion current has little change with increasing pressures because of above opposite effects.

4. CONCLUSIONS

An electrochemical study of pyrite acid pressure oxidation in 0.1 M sulfuric acid was conducted using a self-designed experimental set-up for three-electrode electrochemical measurement in high temperature and high pressure fluids. Open circuit potential, potentiodynamic polarization curves and electrochemical impedance spectroscopy were measured at high temperature (200 - 350 °C) and high pressure (25 - 40 MPa). The following conclusions can be drawn:

(1) At a constant pressure of 40 MPa, the electrode potential decreases with increasing temperatures, indicating that the acid pressure oxidation of pyrite is an exothermic reaction by an electrochemical way.

(2) At 40 MPa, as temperature rises from 200 to 350 °C, i_{corr} increases from 4.33 to 22.16 mA/cm^2, that is, the oxidation rate of pyrite at 350 °C is 5.12 times faster than at 200 °C. The potentiodynamic polarization and EIS studies show that increasing temperature not only accelerate the charge transfer step of acid pressure oxidation of pyrite, but also weaken the passive film at pyrite surface.

(3) Different transfer coefficients and the numbers of electrons transferred in the rate-determining step reveal different electrochemical interaction mechanisms when the temperature increases.

(4) The average activation energy E_a for pyrite oxidation in 0.1 M sulfuric acid in the temperature range of 200 to 350 °C is 29.8 kJ/mol, lower than the results reported in literatures.

(5) At 300 °C, increasing pressures decrease the corrosion potential and the resistance of the charge transfer step, but rarely affects the oxidation rate.

(6) The almost invariable transfer coefficient and number of electrons transferred in the rate-determining step when the pressure increases from 25 to 40 MPa at 300 °C show a constant electrochemical interaction mechanism when the pressure changes.

ACKNOWLEDGMENTS

This work was financially supported by the National Key Research and Development Plan (2016YFC0600100), 135 Program of the Institute of Geochemistry, CAS, and Large-scale Scientific Apparatus Development Program (YZ200720), CAS.

References

1. C. Gasparrini, *CIM Bull*., 76 (1983) 144.
2. V.G. Papangelakis, G.P. Demopoulos, *Can. Metall. Q.*, 29 (1990) 1.
3. O.G. Argall, *Eng. Min. J.*, 187 (1986) 26.
4. H. Long, D.G. Dixon, *Hydrometallurgy*, 73 (2004) 335.
5. D.R. Mckay, J. Halpern, *Trans. Am. Inst. Min. Metall. Eng.*, 212 (1958) 301.
6. L.K. Bailey, E. Peters, *Can. Metall. Q.*, 15 (1976) 333.
7. V.G. Papangelakis, G.P. Demopoulos, *Hydrometallurgy*, 26 (1991) 309.
8. G.H. Kelsall, Q. Yin, D.J. Vaughan, K.E.R. England, N.P. Brandon, *J. Electroanal. Chem.*, 471 (1999) 116.
9. J.D. Rimstidt, D.J. Vaughan, *Geochim. Cosmochim. Acta*, 67 (2003) 873.
10. M.J. Nicol, H. Miki, S. Zhang, P. Basson, *Hydrometallurgy*, 133 (2013) 188.
11. L.J. Bryson, F.K. Crundwell, *Hydrometallurgy*, 143 (2014) 42.
12. A.M. Olmedo, M. Villegas, M.G. Alvarez, *J. Nucl. Mater*., 229 (1996) 102.
13. H. Sun, X.Q. Wu, E.H. Han, *Corros. Sci.*, 51 (2009) 2565.
14. Z.G. Duan, F. Arjmand, L.F. Zhang, F.J. Meng, H. Abe, *J. Solid State Electrochem.*, 19: (2015) 2265.
15. S. Lin, H.P. Li, C. Cui, *Int. J. Electrochem. Sci.* (2016) (accepted).
16. D.D. Macdonald, A.C. Scott, P. Wentrcek, *J. Electrochem. Soc.*, 126 (1979) 1618.
17. J.W. Thompson, T.J. Kaiser, J.W. Jorgenson, *J. Chromatogr. A*, 1134 (2006) 201.
18. A.J. Bard, L.R. Faulkner, Electrochemical Methods Fundamentals and Applications, 2nd Edition, Wiley, (2001) Hoboken, US.
19. X.L. Zhang, Z.H. Jiang, Z.P. Yao, Y. Song, Z.D. Wu, *Corros. Sci.*, 51 (2009) 581.
20. B. Panda, R. Balasubramaniam, G. Dwivedi, *Corrosion Sci.*, 50 (2008) 1684.
21. F. Alcaide, E. Brillas, P.L. Cabot, *J. Electroanal. Chem.*, 547 (2003) 61B.
22. C.H. Hsu, F. Mansfeld, *Corrosion*, 57 (2001) 747.
23. G.Q. L, et. al., Handbook for physical property data of chemistry and chemical engineering-Inorganic volume, Chemical Industry Press, (2001) Beijing, China.
24. Q.Y. Liu, H.P. Li, *Miner. Eng.*, 23 (2010) 691.
25. E.M. Gutman, Mechanochemistry of solid surfaces, World Scientific, (1994) Singapore.
26. Y.G. Yang, T. Zhang, Y.W. Shao, G.Z. Meng, F.H. Wang, *Corros. Sci.*, 73 (2013) 250.
27. H.J. Sun, L. Liu, Y. Li, F.H. Wang, *J. Electrochem. Soc.*, 160 (2013) 89.